# Simulation Analysis and Experimental Study on Vibration Reduction Performance of Groove-Textured Friction Pair Surfaces

Wusheng Tang – Yufei Nie – Zhuo Zhang – Wei Lin – YanKai Rong – Yaochen Shi – Ning Ding ✉
School of Mechanical and Vehicle Engineering, Changchun University, China
✉ 3765750755@qq.com

**Abstract** *To further investigate the influence of surface texture on the vibration characteristics of friction pair surfaces, this study fabricated groove textured on 45# steel surfaces using laser marking technology, forming a friction pair with chloroprene rubber. Numerical analysis of their friction processes under varying speeds was conducted via the finite element analysis software ABAQUS/Explicit (explicit dynamic solver).The results indicate that with increasing speed, the grooved-texture surface enhances its capability to reduce both the intensity and the continuity of contact stress concentration on the friction plate surface, while simultaneously accelerating the diffusion speed of contact stress from the leading edge to the trailing edge of the friction block, thereby better suppressing its concentration at the leading edge. Meanwhile, friction tests were conducted at varying speeds on the HCM-5 reciprocating friction and wear testing machine for the 45# steel-chloroprene rubber friction pair. The results show that at all speeds, the system damping of the freely decaying oscillation component on the surface of the groove texture after "groove-crossing fluctuations" is significantly increased compared to the non-textured surface. As the speed increases, the damping effect of the groove texture on the vibration of the friction pair surface gradually enhances, and the reduction in energy density at the main frequency of the friction pair surface becomes increasingly evident. This corresponds to the numerical analysis results, illustrating the influence of speed on the improvement of the vibration characteristics of the friction pair surface by the groove texture.*

**Keywords** *groove textured, friction characteristics, numerical analysis, velocity*

**Highlights**

- *Groove textures reduce stress concentration at the friction block's front corner.*
- *Groove edges disrupt continuous stress concentration on the friction plate surface.*
- *As speed increases, textures enhance the reduction in stress concentration continuity and intensity.*
- *Groove textures decrease vibration levels on friction surfaces.*
- *Friction surfaces exhibit a dominant frequency of 1116 Hz, with energy density decreasing as speed rises.*

## 1 INTRODUCTION

Relative motion between friction pairs inevitably generates friction and wear. However, in practice, the failure of most mechanical components is not solely caused by friction and wear alone—friction-induced vibration also plays a critical role [1]. Such vibration not only accelerates component wear but may also lead to loosening, fracture, and even systemic instability. Therefore, it is imperative to prioritize vibration issues arising from friction and implement effective damping measures to enhance the stability and reliability of mechanical systems [2-4]. Over the past few decades, surface texturing has gained significant attention as an effective surface modification technique for vibration suppression and stress distribution optimization. By designing specific micro-scale geometric patterns on friction pair surfaces, surface texturing can substantially modify the tribological behavior at the contact interface, thereby reducing vibration, improving stress distribution, and enhancing overall system performance [5-7].

Currently, research on surface texturing primarily employs a combination of experimental studies, numerical simulations, and theoretical analysis. Experimental studies utilize equipment such as friction and wear testers and vibration testing platforms to directly measure the friction coefficient and vibration acceleration of textured surfaces, thereby validating their vibration-damping effects. For instance, experiments have investigated the influence of laser surface texturing on the tribological behavior of gray cast iron [8]. Other studies have experimentally demonstrated the potential of surface texturing in non-metallic sliding-element bearings, revealing its role in reducing friction, minimizing wear, and optimizing lubrication mechanisms [9]. Additionally, experimental research has examined the fretting wear behavior of texture Ti-6Al-4V alloy under oil lubrication [10].

Numerical simulations, including finite element analysis (FEA) and computational fluid dynamics (CFD), model the contact stress, friction force, and vibration characteristics of textured surfaces to uncover underlying mechanisms, often in combination with experimental studies. For example, simulations and experiments have been jointly used to study the friction-reducing effects of fan-shaped surface textures [11]. Similarly, laser-textured surfaces in reciprocating line contacts have been analyzed through combined numerical and experimental approaches to evaluate lubricant film thickness and friction forces [12]. Theoretical analysis involves establishing mathematical models to explore the influence of texture parameters (e.g., shape, size, distribution) on vibration reduction and stress distribution. For instance, theoretical studies have calculated frictional energy dissipation in mechanical contacts under random vibrations [13].

In terms of research objects, studies have primarily focused on metal-polymer friction pairs (e.g., steel-rubber, aluminum-polytetrafluoroethylene (PTFE)). For instance, research has investigated the effect of metal surface texture on the friction and wear

performance of shale oil pumps in highly abrasive media [14], as well as the influence of lead-free bearing materials and surface textures on the performance of sliding bearings [15]. For metal-metal friction pairs (e.g., steel-steel, copper-aluminum), studies have examined the tribological behavior of gradient nanostructures on TB8 titanium alloy surfaces [16], the lubrication performance of femtosecond laser-textured stainless steel surfaces [17], and the tribological properties of single- and multi-shape laser-textured surfaces under dry friction conditions [18]. Study the concentration of stress and strain on gear tooth surfaces and observe the reduction in wear [19]. Metal-polymer pairs have garnered significant attention due to their widespread engineering applications (e.g., bearings, seals). Common surface texture types include micro-dimples, grooves, and wave-like patterns, with groove textures being a research hotspot due to their ease of fabrication and excellent vibration-damping effects. Additionally, the influence of texture parameters (e.g., depth, width, spacing) on vibration reduction and stress distribution remains a key research focus.

In recent years, researchers have proposed various novel mechanisms for surface texturing to reduce vibration and improve stress distribution. For instance, the lubrication theory highlights that surface textures facilitate the formation of lubricating films, thereby reducing friction-induced vibration [20]. Additionally, synergistic mechanisms suggest that the combined effect of textures and lubricants can further enhance wear resistance. For example, the integration of laser texture with solid lubrication has been shown to significantly improve the tribological performance of titanium alloys [21]. Similarly, the synergistic interaction between self-lubricating materials and laser-textured surfaces—such as $MoS_2$ and graphene coatings combined with laser texture—has demonstrated a remarkable enhancement in friction performance [22-23]. Tools with microstructures on both the front and rear cutting edges combined with solid lubricants can effectively improve cutting performance [24].

In summary, extensive research has demonstrated the critical role of surface texturing in reducing friction and wear across various tribological systems. However, existing studies have primarily focused on the dimensional parameters of textures, with limited investigation into how the vibration-damping performance of textured surfaces varies under different sliding velocities. To address this gap, this study employs laser processing to fabricate groove textures on 45# steel surfaces. Using a face-to-face contact configuration with chloroprene rubber (synchronous belt material) as the counter face, reciprocating friction tests are conducted on a HCM-5 tribometer at varying speeds to examine the influence of velocity on the vibration-suppression performance of textured surfaces. Furthermore, explicit dynamic simulations are performed using the finite element software ABAQUS/Explicit to numerically analyze the friction process and validate the experimental findings. This work lays a foundation for the future application of textured surfaces in synchronous belt tensioners.

## 2 METHODS AND MATERIALS

This study employs a combined approach of numerical analysis and experimental research to enhance the accuracy and reliability of the investigation. Firstly, a simulation model is established using numerical analysis to explore the variation patterns of contact stress and friction force in the friction system under different speeds. Secondly, to validate the accuracy of the numerical analysis and investigate subtle differences in practical operation, multiple experiments were designed and conducted to record changes in vibrational acceleration at the friction interface in detail, while comparing and analyzing the results of numerical simulations and actual tests in real time. This approach not only enables timely identification and optimization of potential issues in the numerical model but also accumulates practical experience, thereby enhancing the research's practical value.

### 2.1 Simulation, Numerical Models

The numerical model is designed to simplify the complex three-dimensional system of subsequent experiments into a relatively straightforward three-dimensional model. Its primary purpose is to predict general trends during the experimental process, such as variations in friction force and contact stress on the friction pair surface. The three-dimensional model comprises two main components, as shown in Fig. 1, a friction block and a friction plate (specific dimensional parameters are listed in Table 1). The textured friction plate features groove textured with a spacing of 4000 μm, width of 400 μm, and depth of 30 μm. The figure also illustrates the boundary conditions for the numerical analysis: at $t$ = 0.1 s, a fixed Z-direction load of $F$ = 400 N is applied to the friction block; five degrees of freedom of the friction block are constrained (except for Z-translation); five degrees of freedom of the friction plate are constrained (except for X-translation); a constant translational velocity v is applied along the X-direction; and the friction type is set to "hard" friction with a coefficient of 0.4.

**Table 1. Part Size Parameters**

| Part | $L$ [mm] | $W$ [mm] | $H$ [mm] |
|---|---|---|---|
| Friction block | 20 | 20 | 5 |
| Friction plate | 200 | 50 | 10 |

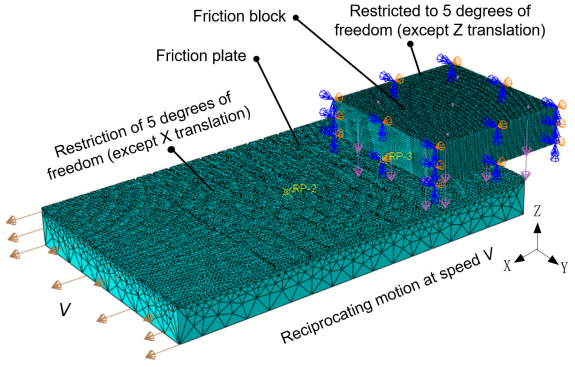


**Fig. 1. Numerical model of friction system**

### 2.2 Experimental

#### 2.2.1 Test Methods and Sample Preparation

To systematically investigate the influence of surface textures on friction performance, this study conducts comparative experiments using multiple sets of data. Smooth surfaces are used as the control group, while textured surfaces serve as the experimental group. During the experiments, consistent texture parameters and loads are maintained, with a focus on comparing the effects of surface textures on friction performance at different speeds. The test conditions are a dry state under atmospheric conditions (temperature: 22 °C to 25 °C). To account for the randomness of the test process, each test group is repeated at least 5 times to ensure accuracy.

The friction plates for both the control group and the experimental group are made of 45# steel, with a hardness of 650 HBS, elastic modulus $E$ = 200 GPa, Poisson's ratio of 0.31, and density of

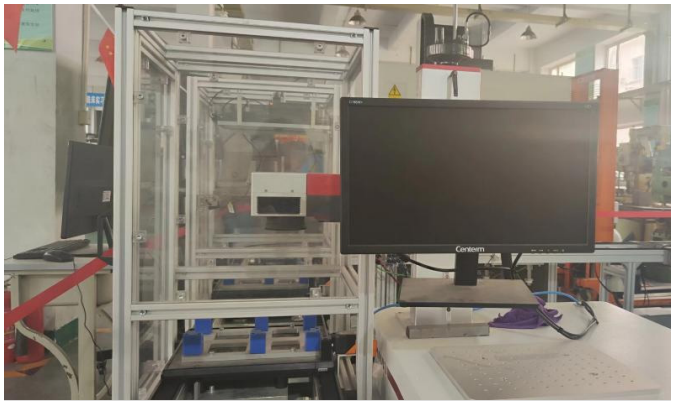

Fig. 2. CX-Q100 laser marking machine

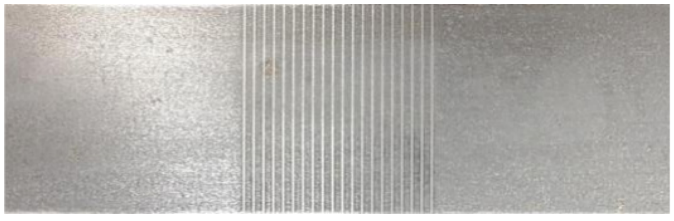

Fig. 3. Friction plate

7850 kg/m³. The surfaces are polished to maintain smoothness. The control group has no texture processing, and the friction plate dimensions are 200 mm × 50 mm × 10 mm, serving as the baseline reference. The experimental group's friction plates are processed with groove textures using a laser marking machine, as shown in Fig. 2, with a depth of 30 μm, width of 400 μm, and spacing of 4000 μm. The actual processed friction plate is shown in Fig. 3. The counter friction blocks are made of chloroprene rubber, with an elastic modulus $E$ = 6 MPa, Poisson's ratio of 0.4, density of 1240 kg/m³, and dimensions of 20 mm × 20 mm × 5 mm.

### 2.2.2 Test Equipment and Parameters

Friction tests at varying speeds for the 45# steel-chloroprene rubber friction pair were conducted using the HCM-5 universal reciprocating friction and wear testing machine. A schematic diagram of the experimental system is shown in Fig. 4a. The testing machine, as shown in Fig. 4b, has a maximum test force of 5000 N, a maximum reciprocating stroke of 200 mm, and a reciprocating frequency range of 1 to 60 cycles/min. Additionally, a KISTLER 3D accelerometer (8763B100AT) is used, with a range of ±100 g, Integrated electronics piezo-electric (IEPE) output sensitivity of 50 mV/g ± 3 mV/g, and a response frequency of 0.5 Hz to 7 kHz, as shown in Fig. 4c. The accelerometer is fixed at 10 mm to 20 mm above the friction plate in the direction of motion. Signal acquisition is performed using the DEWESOFT 8-channel data acquisition system (X-DSA) with a sampling frequency of 10 kHz, as shown in Fig. 4d. During the tests, a constant load of 200 N is applied vertically to the friction block, while the friction plate undergoes reciprocating motion at different speeds: 2 mm/s, 4 mm/s, 6 mm/s, and 8 mm/s, with a reciprocating stroke of 100 mm.

## 3 RESULTS AND DISCUSSION

### 3.1 Simulation results: Contact Stress Analysis of Friction Sub-Surface

The contact interface stress variations when the friction block is positioned at the center of the friction plate ($t$ = 0.5 s) were analyzed, and the numerical results are presented in Fig. 5. The surface contact stress contour maps of the friction block at various speeds for smooth and textured friction pairs are shown in Figs. 5a and b, respectively.

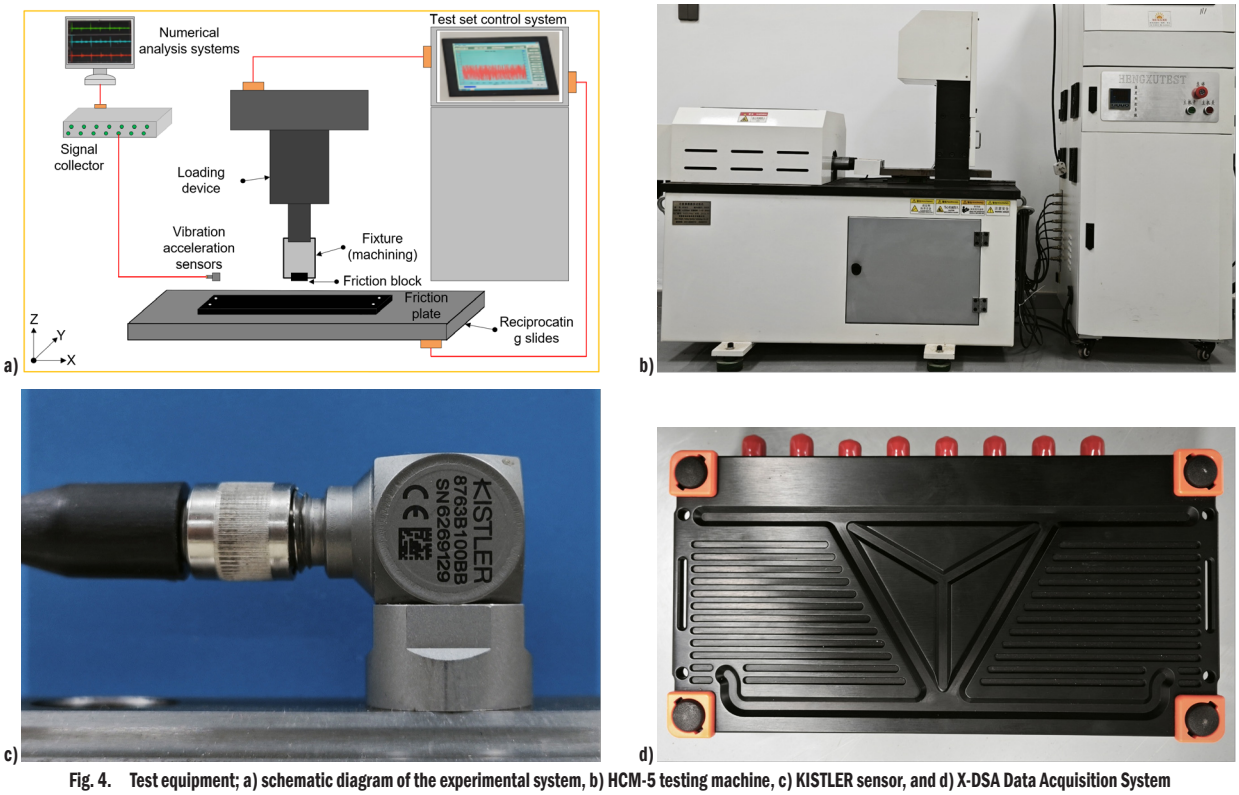


Fig. 4. Test equipment; a) schematic diagram of the experimental system, b) HCM-5 testing machine, c) KISTLER sensor, and d) X-DSA Data Acquisition System

It can be observed that the maximum contact stress in the smooth friction pair is primarily concentrated at the front corner and front edge of the friction block. In contrast, for the textured friction pair, the maximum contact stress is only concentrated at the front corner and shows a tendency to diffuse toward the rear corner, with minimal stress concentration at the front edge. Additionally, the maximum contact stress value decreases from $1.77\times10^{7}$ Pa to $7.97\times10^{5}$ Pa, a reduction of approximately 95.5 %. This demonstrates the role of groove textures in disrupting and dispersing interfacial contact stresses. Moreover, this effect becomes more pronounced as speed increases, as the diffusion of stress from the front to the rear corner accelerates.

To more intuitively observe the effect of groove texture edges, Figs. 5c and d show the contact stress contour maps of smooth and textured friction plate surfaces at various speeds. Significant stress concentrations are observed on all smooth surfaces, but as speed increases, the continuity and intensity of these concentrations decrease noticeably, as seen at points 1, 2, and 3 in Fig 5. Although the concentration intensity increases slightly when speed rises from 2 mm/s to 4 mm/s, the stress concentration at point 4 has already disappeared. Overall, as speed increases, both the area and intensity of stress concentration on smooth surfaces gradually decrease.

Similarly, as shown in Fig. 5d, the contact stress contour maps of the textured friction plate surface reveal that, compared to the smooth surface, the maximum contact stress decreases from $1.099\times10^{6}$ Pa to $4.885\times10^{5}$ Pa, a reduction of approximately 55.56 %, with an overall significant decrease in stress values. Furthermore, at various speeds, as indicated at points 5, 6, 7, and 8 in the Fig 5d, high-intensity stress concentrations are significantly reduced compared to the smooth surface, and this reduction trend is proportional to speed. This demonstrates that groove textures effectively reduce stress concentration and intensity at all speeds, and overall, the effect becomes more pronounced as speed increases.

### 3.2 Simulation results: Friction Analysis of Friction Sub-Surfaces

To further observe the "disruptive" effect of groove textures, the friction force on the friction plate surface over time at various speeds (with a friction coefficient of 0.6 for smooth surfaces and 0.4 for textured surfaces) is obtained through numerical analysis, as shown in Figs 6a and b. Firstly, all figures exhibit fluctuations in friction force caused by collisions between the edges of the friction block and the groove textures (as shown in the magnified views at point 1 in each figure). At speeds of 2 mm/s to 8 mm/s, the fluctuation ranges are approximately ±10 N, ±20 N, ±23 N, and ±26 N, respectively. This is because, during the collision process, the system's momentum is conserved, meaning the total momentum of the system remains constant before and after the collision. The higher the speed, the greater the momentum of the object, resulting in a larger impact force during collisions and more pronounced fluctuations in friction force. However, as the friction block continues to slide, the friction force returns to its previous level due to the area loss caused by the grooves. It is precisely this intermittent friction state that achieves

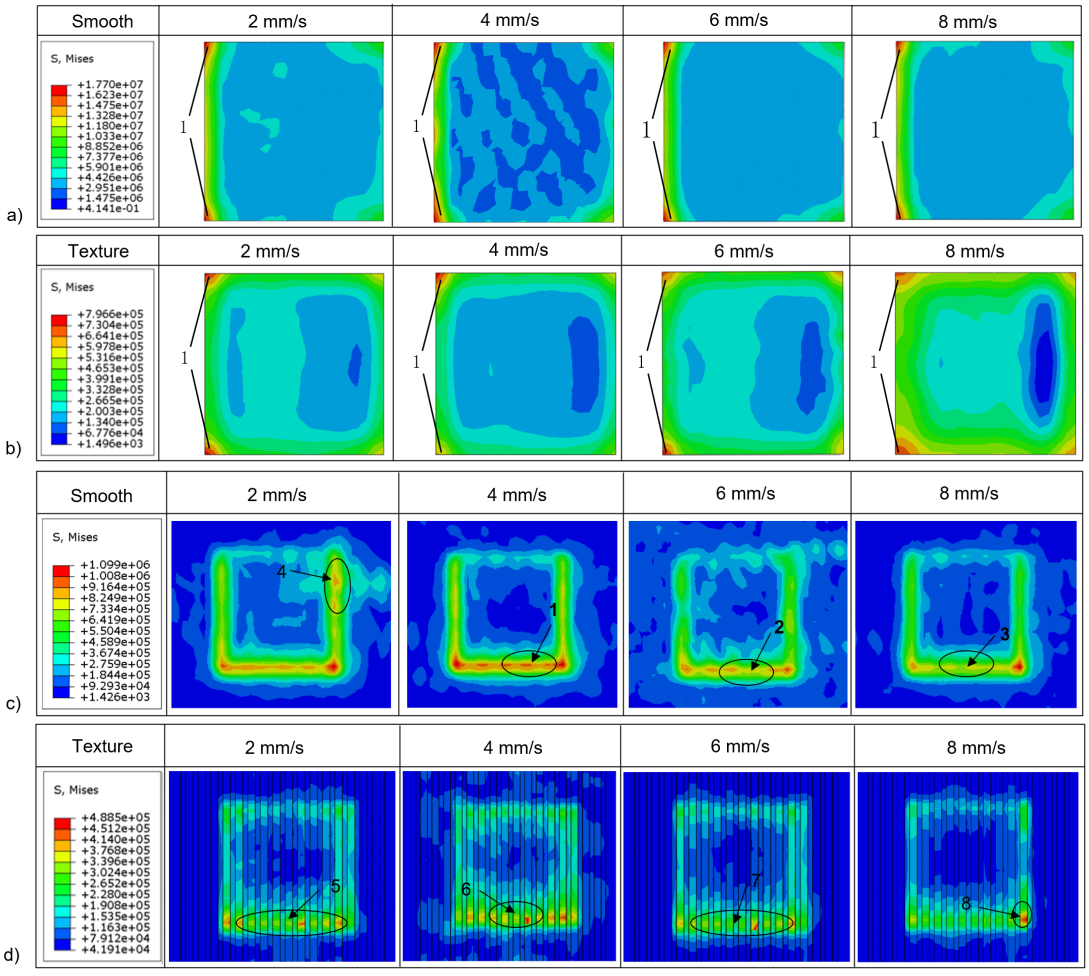


**Fig. 5. Contact stress contour maps; a) smooth-friction block, b) textured friction block, c) smooth-friction plate, and d) textured-friction plate**

the goal of suppressing contact stress concentration on the friction pair surface, thereby preventing sustained vibrations in the friction system. Secondly, due to differences in speed, the frequency of edge collisions varies. Although higher speeds result in higher frequencies and more pronounced "disruptive" effects, they also imply greater impacts. Therefore, analyzing the vibrations of the friction system is essential.

### 3.3 Test Results: Time-Domain Analysis of Vibration Acceleration

Due to the presence of groove edges, the friction force can momentarily surge, which may lead to increased damping in the system during motion, thereby reducing vibration acceleration. Conversely, a decrease in friction force may result in increased vibration acceleration. In reciprocating friction tests, the periodic variation of friction force can cause periodic fluctuations in the vibration acceleration of the friction surface, directly affecting the amplitude and frequency of these fluctuations. Therefore, analyzing the vibration acceleration of the friction surface is essential. The average vibration acceleration amplitudes in three directions for groove-textured friction surfaces at different relative speeds are shown in Fig. 7. It is evident that at all speeds, the average amplitude in the Z-direction (normal to the groove edges) is significantly larger than those in the Y-direction (parallel to the groove edges) and X-direction (perpendicular to the groove edges). This is because the Z-direction is the load application direction during friction, making the friction force changes most pronounced during impacts, leading to more surface vibrations. Furthermore, as shown in Fig. 7b, the

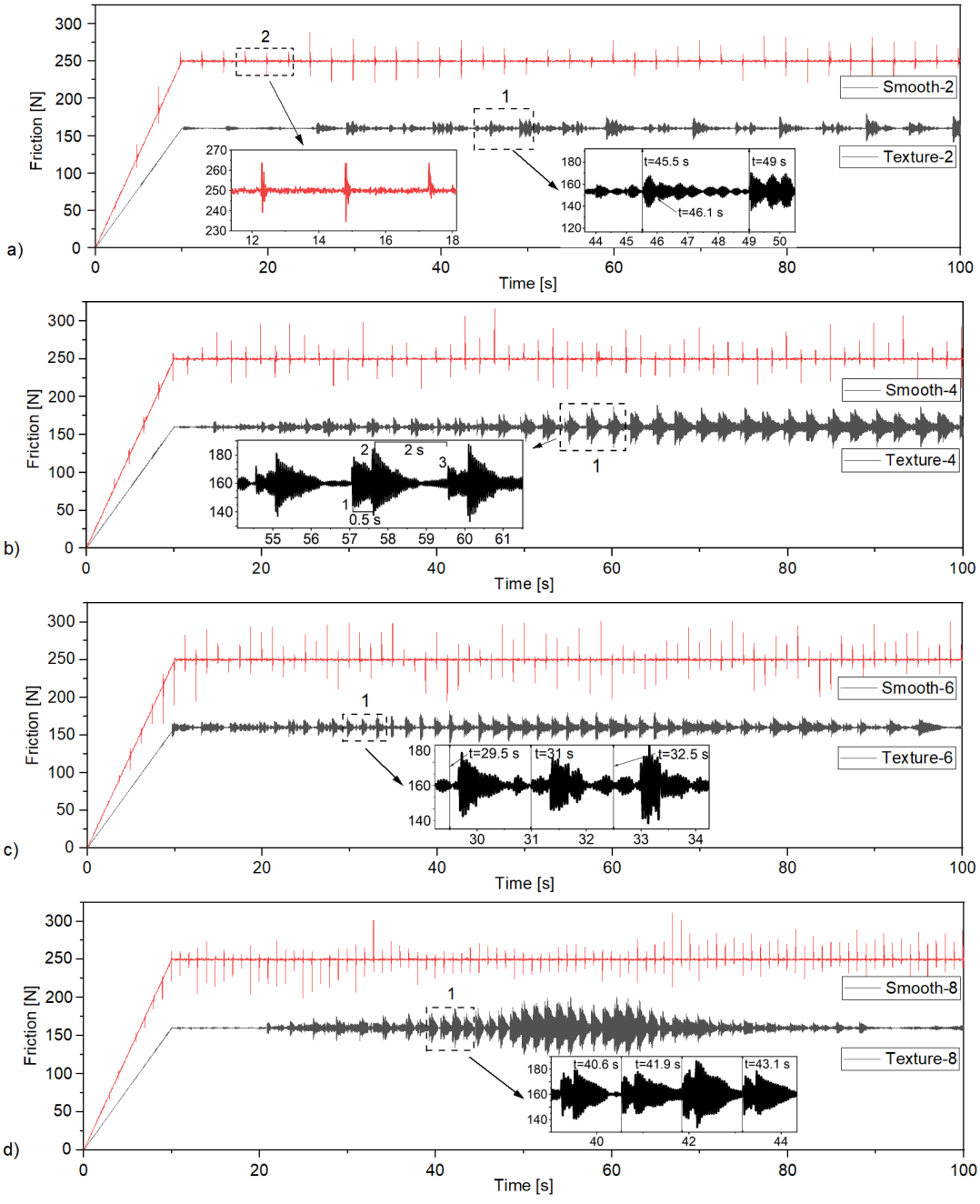


**Fig. 6. Friction time-domain diagram at different velocities: a) 2 mm/s, b) mm/s, c) 6 mm/s, and d) 8 mm/s**

variation trends of the average amplitudes in the three directions are highly consistent with speed changes. Therefore, this study primarily focuses on analyzing the Z-direction, where the vibration acceleration signal changes are most significant.

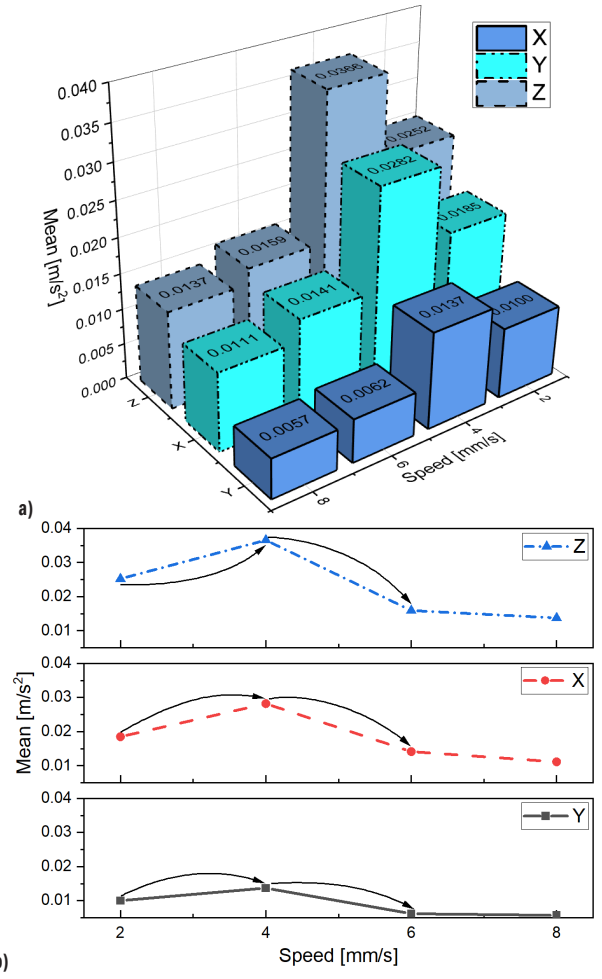


**Fig. 7. Mean value of vibration acceleration; a) three-dimensional, and b) line graphs**

The time-domain graph of the Z-direction vibration acceleration signals of the surface of the belt textured in two cycles at each speed is shown in Fig. 8a, which is processed by the short-time Fourier transform as well as its inverse transformation with low-pass filtering. From 0 to T1 is the friction block going, T1 to T2 is the friction block returning, and after T2 is the second reciprocal cycle.

In the low-speed stage (2 mm/s), the system may be in a static friction-dominated state with significant periodic stick-slip effects, and although there is relative motion in the macroscopic view, there may be intermittent sticking and sliding, or stick-slip phenomenon, in the microscopic level. However, when the speed is increased to 4 mm/s, the system is in the critical region of the transition from static friction to dynamic friction. The dynamic change of friction (static friction alternating with dynamic friction) is the most intense, resulting in a concentrated release of vibration energy and the formation of amplitude peaks. At higher speeds (6 mm/s to 8 mm/s), dynamic friction dominates, sliding tends to be continuous and stable, and the stick-slip effect is weakened. Therefore, the amplitude fluctuation is most obvious when the speed is 4 mm/s from the point of view of the overall amplitude of acceleration.

Figure 8b provides a magnified view of region 1 in Fig. 8a. The positions marked as G1 to G2 in the figure represent the amplitude surges caused by edge impacts at each speed, referred to as "groove-crossing fluctuations" These fluctuations are prominent at 6 mm/s and 8 mm/s, while at 2 mm/s, the impact is minimal due to the slower groove-crossing speed. However, at 4 mm/s, in addition to the groove-crossing fluctuations caused by edge impacts, there are also amplitude surges marked at positions I and II, which occur when passing over the non-textured surface due to vibrations. Although vibrations are present on the non-textured surface at other speeds, the amplitude surges at positions I and II demonstrate that the vibration intensity is significantly lower compared to that at 4 mm/s.

$$\delta = \frac{1}{k}\ln\left(\frac{X_n}{X_{n+k}}\right), \tag{1}$$

$$\zeta = \frac{\delta}{\sqrt{4\pi^2+\delta^2}}. \tag{2}$$

To observe the damping effect of the grooves more obviously, the free decaying oscillating part (I-II) after the "groove-crossing fluctuations" at each speed is targeted. The damping ratios were calculated according to Eqs. (1) and (2) and compared with the non-texture surface, where $X_n$ and $X_{n+k}$ are the peaks separated by $k$ cycles, and if $k=1$, it means the adjacent peaks, and $\delta$ is the logarithmic decreasing amount. The damping ratios of I-II positions at each velocity are in order $\zeta_{2(\text{I-II})}\approx 0.5674$, $\zeta_{4(\text{I-II})}\approx 0.1587$, $\zeta_{6(\text{I-II})}\approx 0.5734$, $\zeta_{8(\text{I-II})}\approx 0.5884$. The damping ratios of the non-woven surface at each speed are $\zeta_{2(n-t)}\approx 0.1441$, $\zeta_{4(n-t)}\approx 0.1248$, $\zeta_{6(n-t)}\approx 0.1341$, and $\zeta_{8(n-t)}\approx 0.1178$. At a speed of 4 mm/s, the system damping after passing through the groove increased by approximately 21.3 % compared to the non-textured surface, while at other speeds, the damping increased by nearly 75 % compared to the non-textured surface, indicating that texture can improve the vibration level of the surface at all speeds.

And if we want to further assess the change rule of groove vibration damping ability with velocity, it is inaccurate to use only the change of damping ratio after passing the groove. So, the mean value of the amplitude when the friction block passes through the non-textured surface was calculated, to visualize the effect of velocity on the vibration damping effect of the groove textured.

Thus, the vibration acceleration data during the $t_1-t_2$ period when the friction block passes over the non-textured surface at each speed were extracted to calculate the average values, which were then compared with those of the smooth surface. The results are shown in Fig 9a. At speeds of 2 mm/s to 8 mm/s, the average values for the non-textured surface are 0.02897 m/s², 0.05132 m/s², 0.03245 m/s², and 0.03479 m/s², respectively, while the corresponding values for the smooth surface are 0.03484 m/s², 0.06391 m/s², 0.04296 m/s², and 0.04828 m/s². Therefore, as speed increases, the vibration of the friction surface gradually intensifies, which is directly related to the "groove-crossing fluctuations" of friction force observed in the numerical analysis—higher speeds result in larger fluctuations. However, compared to the smooth surface, the average amplitudes of the textured surface are all reduced. The reduction percentages are shown in Fig 9b at speeds of 2 mm/s to 8 mm/s, the reductions are 16.81 %, 19.69 %, 24.46 %, and 27.94 %, respectively. This demonstrates that as speed increases, the vibration damping capability of groove textures gradually improves, which is highly consistent with the enhanced disruption of contact stress concentration observed in the numerical analysis.

### 3.4 Test Results: Frequency-Domain Analysis of Vibrational Acceleration

Through short-time Fourier transform and filtering processing of the time-domain vibration acceleration signals, the frequency-domain diagram shown in Fig. 10 was obtained. Firstly, the Z-direction

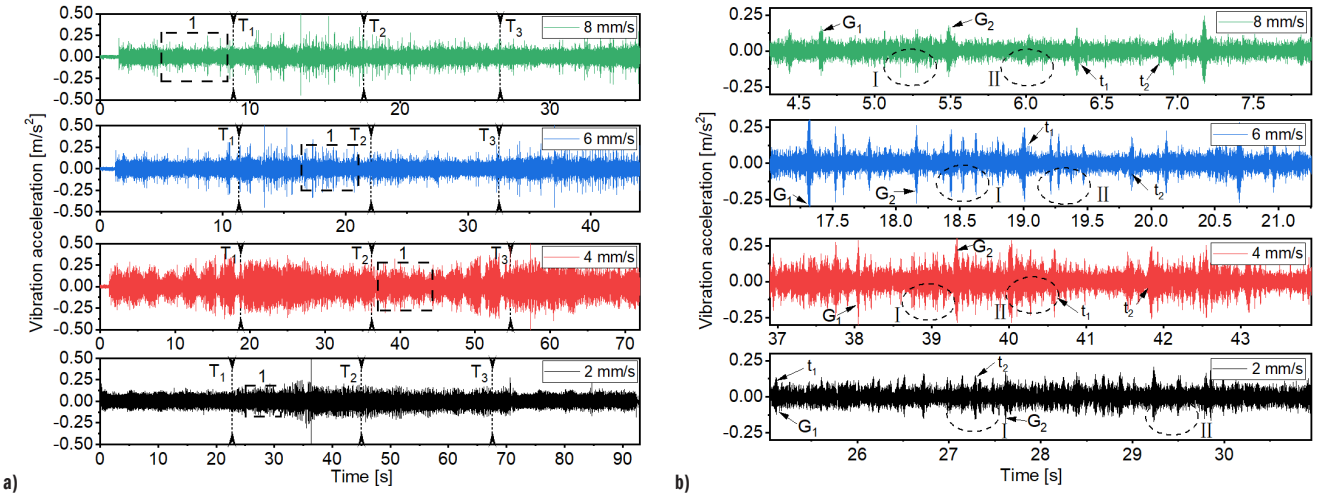


Fig. 8. Time-domain of vibration acceleration; a) of texture surfaces, and b) at enlargement at "1"

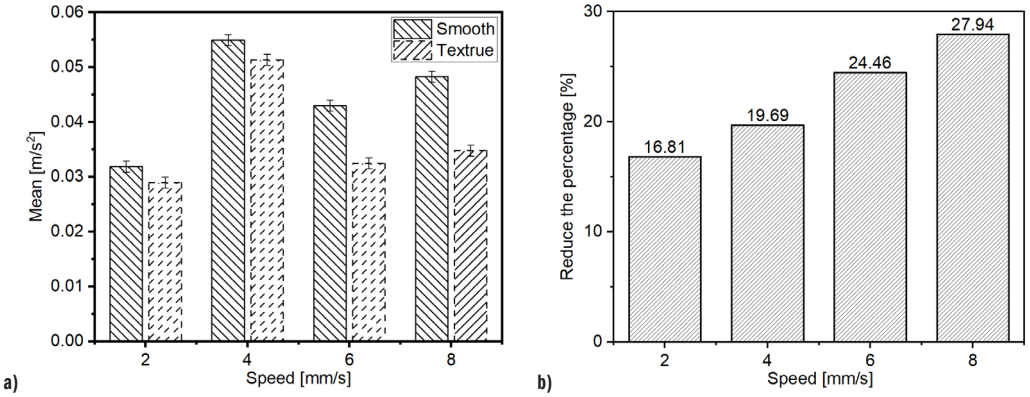


Fig. 9. The mean value of vibration acceleration; a) Average amplitude, and b) percentage reduction

vibration acceleration of friction surfaces at all speeds exhibited a dominant frequency around 1116 Hz. This dominant frequency is generally associated with the system's natural frequency or external excitation frequency, and therefore remains stable without changing with speed variations.

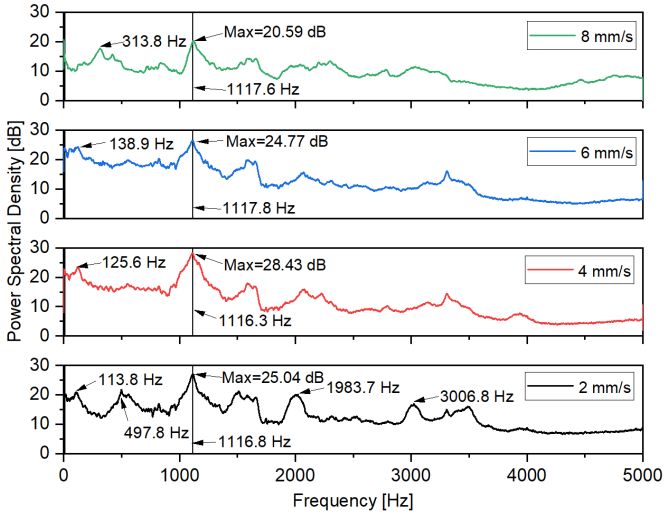


Fig. 10. Frequency-domain analysis of vibration acceleration

Secondly, comparative analysis of energy density at the dominant frequency under different speeds reveals specific values: 25.04 dB at 2 mm/s, 28.43 dB at 4 mm/s, 24.77 dB at 6 mm/s, and 20.59 dB at 8 mm/s. Overall, the energy suppression effect of groove texture at the dominant frequency enhances with increasing speed.

Additionally, all speed conditions exhibited elevated energy levels in low-frequency ranges (113.8 Hz, 125.6 Hz, 138.9 Hz, and 313.8 Hz) induced by the groove texture. These frequency components directly correlate with friction fluctuations and amplified vibration amplitudes resulting from collisions between the friction block and groove edges. As speed increases, the collision frequency accelerates, consequently shifting the energy concentration frequencies associated with groove edge impacts to higher values.

## 4 CONCLUSIONS

To investigate the influence of speed on the improvement of vibration characteristics of friction pair surfaces by groove textures, this study combines numerical analysis and experimental research to analyze the variations in contact stress, friction force, and vibration acceleration on the friction surface at different speeds. The following conclusions are drawn:

Firstly, numerical analysis verifies that, at all speeds studied, groove textures can diffuse the concentration of contact stress from the front corner to the rear corner of the friction block, thereby suppressing excessive concentration at the front corner. Simultaneously, the presence of groove edges disrupts and disperses the contact stress on the friction plate surface, reducing its concentration intensity and continuity. Compared to the smooth

surface, the maximum contact stress decreases from $1.099 \cdot 10^6$ Pa to $4.885 \cdot 10^5$ Pa, a reduction of approximately 55.56 %.

Secondly, as speed increases, the diffusion of contact stress from the front corner to the rear corner of the friction block accelerates. The effectiveness of groove textures in reducing the continuity and intensity of stress concentration on the friction surface gradually improves. By analyzing the variations in friction force at different speeds, the differences in the "disruptive" effect of groove edges are validated.

The final test shows that, in the time domain analysis of the surface vibration of the friction sub-surface, the system damping of the freely decaying oscillating part of the groove surface after the "groove-crossing fluctuations"at a speed of 4 mm/s increases by 21.3 % compared with the non-textured surface, and the increase in the rest of the speed is up to 75 %. The mean value of the acceleration amplitude on the grooved surface was lower than that on the non-textured surface at the same velocity, and the decrease was positively correlated with the velocity. Frequency domain analysis shows that the dominant frequency of all surfaces is around 1116 Hz, but due to the effect of "groove-crossing fluctuations", there is a low-frequency high-energy density region at different speeds. The main frequency energy density decreases with the increase of speed, which confirms that increasing the speed is conducive to improving the vibration characteristics of the groove structure, verifying the numerical analysis of the law, and laying a foundation for the application of synchronous belt tensioning wheel.

## References


[1] Braun, D.,Greiner, C.,Schneider, J., Gumbsch, P. Efficiency of laser surface texturing in the reduction of friction under mixed lubrication. *Tribol Int* 77 142-147 (2024) **DOI:10.1016/j.triboint.2014.04.012**.

[2] Prem Ananth, M., Poovazhagan, L., Risikesh, J., Tanari, S.V., Sidheswaren, J. Tribological behaviour of titanium alloy due to surface modification technique. *Int J Surf Sci Eng* 18 130-148 (2024) **DOI:10.1504/ijsurfse.2024.138503**.

[3] Wang, D.W., Mo, J.L., Liu, M.Q., Li, J.X., Ouyang, H., Zhu, M.H. et al. Improving tribological behaviours and noise performance of railway disc brake by grooved surface texturing. *Wear* 376-377 1586-1600 (2017) **DOI:10.1016/j.wear.2017.01.022**.

[4] Wang, D.W., Mo, J.L., Zhu, Z.Y., Ouyang, H., Zhu, M.H., Zhou, Z.R. How do grooves on friction interface affect tribo-logical and vibration and squeal noise performance. *Tribol Int* 109 192-205 (2017) **DOI:10.1016/j.triboint.2016.12.043**.

[5] Yang, S., Song, Z., Tong, X., Han, P. Study on the friction noise behaviour of coating textured surface based on STFT time-frequency analysis. *Int J Surf Sci Eng* 17 295-316 (2023) **DOI:10.1504/ijsurfse.2023.135788**.

[6] Wang, A.Y., Mo, J.L., Qian, H.H., Wu, Y.K., Xiang, Z.Y., Chen, W. et al. The effect of a time-varying contact surface on interfacial tribological behaviour via a surface groove and filler. Wear 478-479 203905 (2021) **DOI:10.1016/j.wear.2021.203905**.

[7] Zhang, D., Zhao, F., Wei, X., Gao, F, Li, P., Dong, G. Effect of texture parameters on the tribological properties of spheroidal graphite cast iron groove-textured surface under sand-containing oil lubrication conditions. *Wear* 428-429 470-480 (2019) **DOI:10.1016/j.wear.2019.04.015**.

[8] Kumar, B.A., Babu, P.D., Marimuthu, P., Duraiselvam, M. Effect of laser surface texturing on tribological behaviour of grey cast iron. *Int J Surf Sci Eng* 13 220-235 (2019) **DOI:10.1504/ijsurfse.2019.102381**.

[9] El Fahham, I.M.,Massoud, I.M.. El Gamal, H.A. Performance of non-metallic sliding element textured bearing. *Int J Surf Sci Eng* 16 1-16 (2022) **DOI:10.1504/ijsurfse.2022.122180**.

[10] Cao, W., Hu, T., Fan, H., Ding, Q., Hu, L. Fretting behaviour of textured Ti-6Al-4V alloy under oil lubrication. *Int J Surf Sci Eng* 15 165-164 (2021) **DOI:10.1504/ijsurfse.2021.118199**.

[11] Wei, Y., Yan, H., Li, S., Wang, X. Numerical and experimental study of a sector-shaped surface texture in friction reduction. *Tribol Lett* 72 60 (2024) **DOI:10.1007/s11249-2024-01863-3**.

[12] Vlădescu, S.-C., Medina, S., Olver, A.V., Pegg, I.G., Reddyhoff, T. Lubricant film thickness and friction force measurements in a laser surface textured reciprocating line contact simulating the piston ring-liner pairing. *Tribol Int* 98 317-329 (2016) **DOI:10.1016/j.triboint.2016.02.026**.

[13] Aleshin, V.V., Papangelo, A. Friction-induced energy losses in mechanical contacts subject to random vibrations. *Int J Solids Struct* 190 148-155 (2020) **DOI:10.1016/j.ijsolstr.2019.10.026**.

[14] Janssen, A., Pinedo, B., Igartua, A., Guido Liiskmann, Sexton, L. Study on friction and wear reducing surface micro-structures for a positive displacement pump handling highly abrasive shale oil. *Tribol Int* 107 1-9 (2017) **DOI:10.1016/j.triboint.2016.11.017**.

[15] Sharma, V.K., Singh, R.C., Chaudhary, R. Improvement in the performance of journal bearings by using lead-free bearing material and surface texturing. *Int J Surf Sci Eng* 14 238-256 (2020) **DOI:10.1504/ijsurfse.2020.110542**.

[16] Liu, Y., Cui, H., Pan, S., Xia, Y., Zhao, X. Study on the tribological behaviour of surface gradient nanostructure in TB8 titanium alloy. *Int J Surf Sci Eng* 16 238-257 (2022) **DOI:10.1504/ijsurfse.2022.125457**.

[17] Wang, Z., Li, Y., Bai, F. Wang, C., Zhao, Q. Angle-dependent lubricated tribological properties of stainless steel by femtosecond laser surface texturing. *Opt Laser Technol* 81 60-66 (2016) **DOI:10.1016/j.optlastec.2016.01.034**.

[18] Zhan, X.,Yi, P., Liu, Y., Xiao, P., Zhu, X., Ma, J. Effects of single- and multi-shape laser-textured surfaces on tribological properties under dry friction. *P I Mech Eng C-J Mec* 234 1382-1392 2020 **DOI:10.1177/0954406219892294**.

[19] Xu, T., Guan, Q., Ma, C. The Impact of Micro-texture Distribution on the Frictional Performance of Straight Bevel Cylindrical Gears. *Stroj vestn-J Mech E* 70 582-594 (2024) **DOI:10.5545/sv-jme.2024.1033**.

[20] Uddin, M.S., Liu, Y.W. Design and optimization of a new geometric texture shape for the enhancement of hydrodynamic lubrication performance of parallel slider surfaces. *Biosurf Biotrib* 2 59-69 (2016) **DOI:10.1016/j.bsbt.2016.05.002**.

[21] Cao, W., Hu, T., Fan, H., Hu, L. Laser surface texturing and tribological behaviour under solid lubrication on titanium and titanium alloy surfaces. *Int J Surf Sci Eng* 15 50-66 (2021) **DOI:10.1504/ijsurfse.2021.114347**.

[22] Hua, X., Puoza, J.C., Zhang, P., Sun, J. Friction properties and lubrication mechanism of self-lubricating composite solid lubricant on laser textured AISI 52100 surface in sliding contact. *Int J Surf Sci Eng* 12 228-246 (2018) **DOI:10.1504/ijsurfse.2018.094774**.

[23] Arenas, M.A., Ahuir-Torres, J.I., García, I, Carvajal, H, de Damborenea, J. Tribological behaviour of laser textured Ti6Al4V alloy coated with MoS2 and graphene. *Tribol Int* 128 240-247 (2018) **DOI:10.1016/j.triboint.2018.07.031**.

[24] Zhang, Y., Sun, H., Li, Q., Sun, K., Mou, Y. and Zhang, S. Research on the cutting performance of self-lubricating tools with microtexture of the front and back surfaces. *Stroj vestn-J Mech E* 71 136-145 (2025) **DOI:10.5545/sv-jme.2024.1181**.


**Acknowledgements** *This work was supported by the Natural Science Foundation of Jilin Province, the Provincial-Terrestrial Cooperation Fund Project (No.:YDZJ202401325ZYTS) and the 20th Innovative and Entrepreneurial Talent Funding Program of Jilin Province.*

**Received: 2024-11-06, revised: 2025-03-28, 2025-05-11, accepted: 2025-05-28** *as Original Scientific Paper.*

**Data Availability** *The data that support the findings of this study are available from the corresponding author upon reasonable request.*

**Author contribution** *Wusheng Tang: Project administration, Funding acquisition; Yufei Nie: Validation, Data curation, Writing - review & editing; Zhuo Zhang: Formal analysis, Validation, Writing - original draft, Wei Lin: Conceptualisation, Methodology, Writing - review & editing; Yankai Rong: Data curation, Project administration; Yaochen Shi: Supervision, Methodology, Writing - review & editing; Ning Ding: Methodology, writing - review & editing. All authors made significant contributions to this work andthoroughly reviewed and approved the final version of the manuscript.*

## Numerična in eksperimentalna raziskava vpliva teksture z utori na zmanjšanje vibracij kontaktnih površin

**Povzetek** *Za podrobnejše raziskovanje vpliva površinske teksture na vibracijske značilnosti površin kontaktnega para je bila v tej študiji izdelana tekstura z utori na površini jekla C45 s tehnologijo laserskega označevanja, ki je bila uporabljena v kontaktnem paru s kloroprensko gumo. Numerična analiza trenja med površinama pri različnih hitrostih je bila izvedena z eksplicitno dinamično analizo v programskem paketu ABAQUS/Explicit. Rezultati kažejo, da z naraščajočo hitrostjo med kontaktnimi površinami, uporaba teksture z utori zmanjša intenzivnost in zveznost koncentracije kontaktnih napetosti ter hkrati pospešuje prehod kontaktnih napetosti od vstopnega roba proti izstopnemu robu kontakta, kar učinkovito zmanjša koncentracijo napetosti na vstopnem robu. Eksperimentalni preizkusi trenja med jeklom C45 in kloroprensko gumo pri različnih hitrostih so bili izvedeni z izmeničnim gibanjem na preizkusnem stroju za trenje in obrabo tipa HCM-5. Rezultati kažejo, da se pri vseh hitrostih, dušenje prostega pojemajočega nihanja na površini z utori po »nihanjih ob prečkanju prehodov« bistveno poveča v primerjavi z gladko površino. Z naraščanjem hitrosti se dušilni učinek teksture z utori na vibracije kontaktnih površin postopno krepi, zmanjševanje gostote energije pri glavni frekvenci vibracij pa postaja vse bolj izrazito. To sovpada z rezultati numeričnih analiz in kaže na vpliv hitrosti na zmanjšanje vibracij kontaktnih površin z uporabo teksture z utori.*

**Ključne besede** *tekstura z utori, trenje, numerična analiza, hitrost*